Optimizing Energy Management for Full-Electric Vessels

A Health-Aware Approach with Hydrogen and Diesel Employing Equivalent Consumption Minimization Strategy

Loffler, Charlotte; Kopka, Timon; Geertsma, Rinze; Polinder, Henk; Coraddu, Andrea

Citation (APA)
Loffler, C., Kopka, T., Geertsma, R., Polinder, H., & Coraddu, A. (2024). Optimizing Energy Management for Full-Electric Vessels: A Health-Aware Approach with Hydrogen and Diesel Employing Equivalent Consumption Minimization Strategy. In *Proceedings of the IEEE Transportation Electrification Conference and Expo, Asia-Pacific, ITEC Asia-Pacific 2023* IEEE. https://doi.org/10.1109/ITECAsia-Pacific59272.2023.10372270

Important note
To cite this publication, please use the final published version (if applicable).
Please check the document version above.

Optimizing Energy Management for Full-Electric Vessels: A Health-Aware Approach with Hydrogen and Diesel Employing Equivalent Consumption Minimization Strategy

1st Charlotte Löffler
Maritime and Transport Technology
Delft University of Technology
Delft, Netherlands
c.loeffler@tudelft.nl

2nd Timon Kopka
Maritime and Transport Technology
Delft University of Technology
Delft, Netherlands
t.kopka@tudelft.nl

33rd Rinze Geertsma
Maritime and Transport Technology
Delft University of Technology
Delft, Netherlands
r.geertsma@tudelft.nl

4th Henk Polinder
Maritime and Transport Technology
Delft University of Technology
Delft, Netherlands
h.polinder@tudelft.nl

5th Andrea Coraddu
Maritime and Transport Technology
Delft University of Technology
Delft, Netherlands
a.coraddu@tudelft.nl

Abstract—The path to zero-emission shipping is deeply connected to full-electric vessels. One major challenge to enable this technology for broader application is the design of optimal energy management (EM). The flexibility of operating load sharing in hybrid energy systems could lead to suboptimal solutions using rule-based control. Advanced control strategies can be used to find optimal solutions for the EM problem. In addition, the use of advanced control allows for the incorporation of multiple objectives. An important compromise is the decision between minimizing cost and emissions. A promising approach for EM is the Equivalent Consumption Minimization Strategy (ECMS), which allows for instantaneous optimization of the problem and is suitable for dealing with fast system dynamics. The strategy assigns equivalent factors in the objective function, leading to an easily expandable multi-objective control approach.

This paper presents a novel ECMS-based control strategy for health-aware EM of a full-electric vessel, incorporating diesel internal combustion engines, fuel cells, and batteries with flexible changing operation conditions. To this aim, firstly, we introduce our innovative formulation of the multi-objective problem, considering fuel and electricity expenditures and CO_2 and NO_x emissions, alongside the degradation of batteries and fuel cells. Subsequently, we determine the equivalent factors by employing a Pareto Front approach. Lastly, our developed controllers are assessed against a benchmark derived from state-of-the-art strategies. A case study of a full-electric vessel showcase the potential of our proposed solution. The results demonstrate the control's effectiveness in optimizing the operation considering a variety of objectives, such as fuel consumption or emission production, under variable operational conditions.

Index Terms—Energy Management, Full-Electric Vessel, Alternative Fuels, ECMS, NOx Emission

I. INTRODUCTION

Full-electric vessels are important for transitioning to a sustainable maritime industry [1]. Electrified shipboard power systems allow the integration of various power generation and storage components into the energy system, resulting in increased operational flexibility. This can lead to a more energy-efficient operation and decreased CO2 emissions [2]. However, the increased complexity of those heterogeneous energy systems could lead to suboptimal control solutions using rule-based control (RBC) when trying to optimize for multiple targets at the same time [3]. While an RBC can be highly effective and cost-effective for single objective control, a focus on heterogeneous objectives, sometimes also contradicting, renders this control approach more and more infeasible. Multi-objective control is increasingly necessary to operate energy systems incorporating several power sources successfully. Advanced control strategies allow for multi-objective optimization of fuel consumption (SFC), emission output, and degradation of power generation components simultaneously [4].

A simple way to realize zero-emission full-electric vessel propulsion is to use battery-only systems [5]. However, the low energy density of the battery limits the application to short travel distances of the vessel without recharging [6]. To maintain the autonomous travel distance while decreasing the emission output of a diesel-fuelled vessel, alternative fuels gain more importance [5]. Alternative fuels for application in internal combustion engines (ICE) or fuel cells (FC) have been researched for integration into marine energy systems in the past years [7]. However, both FC and hydrogen come

with high costs, which can restrict their practical application. A combination with diesel or alternatively fuelled ICE could allow for cost- and energy-efficient operation at high loads. In ICE, alternative fuels can significantly reduce emissions [8].

However, one problem of FC and batteries is the degradation of the components [9]. Health-aware control strategies incorporate factors relating the component's degradation to the operation [10]. While the aspect of battery aging is addressed quite frequently in the automotive industry [11], the combination of FC and battery aging is a relatively new field of research. Incorporating health-awareness into a multi-objective problem that addresses cost and emissions further complicates the control challenge. When integrating a dual fuel system, the control mechanism faces a trade-off: opting for diesel, a more cost-effective fuel that unfortunately results in CO_2 and NOx emissions, or for hydrogen, which, while being emission-free, is costlier and accelerates the degradation of the FC. Furthermore, when integrating these power sources with an energy storage system like batteries, one gains the advantage of buffering against load variations and achieving peak shaving. However, this integration concurrently introduces an operational-dependent battery degradation as an objective. Consequently, this situation results in a multi-objective optimization problem requiring a real-time solution to guarantee optimal vessel operation.

The current state of marine energy management research rarely considers more than two objectives simultaneously. Predominantly, these objectives are fuel consumption, viewed as a primary cost determinant, and CO2 production, targeted for emission mitigation. Some researchers also incorporated battery aging [12] and FC aging [9]. However, some challenges remain still unaddressed. One is the emission reduction, which needs to consider other emissions besides CO_2 as well due to rising restrictions in many areas. NOx emissions are not related to the SFC but to the local temperatures and air-fuel mixture composition in the ICE, which are determined by its operating point. However, the emission reduction aspect gets more complex in a dual fuel scenario when the decision is to be made between increased cost and degradation for a zero-emission fuel in an FC and the emissions from an ICE. The most optimal point of operation can vary between different operation types and locations. This gap requires further research.

Advanced control strategies have been extensively researched for marine energy management. Among these, Model Predictive Control (MPC) stands out as a notable approach for improving energy efficiency in various application fields with a predictable operating profile [13], including the maritime. MPC can be used for energy management with various objectives [14]. However, one major problem of MPC is the required knowledge of the system [15]. Especially for vessels with a high degree of uncertainty in the load profile, the application of MPC is difficult. A promising advanced control strategy is Equivalent Consumption Minimization (ECMS). ECMS has garnered significant attention in automotive research. Owing to analogous problem characteristics, it exhibits considerable

potential for application in the maritime sector.

The ECMS method is commonly employed to minimize consumption between components such as engines, fuel cells, and batteries. Significantly, ECMS's can account for component aging as an objective, as shown by Li et al. [16]. Intrinsically, ECMS correlates objectives via equivalent factors for battery use within its objective function. This correlation empowers the control mechanism to strike an optimal balance among objectives of varying natures. ECMS serves as a real-time control strategy, offering computational and temporal efficiencies over the MPC. In a pioneering maritime application, Kalikatzarakis et al. [17] have underscored the fuel-saving capabilities of ECMS. Nevertheless, the holistic integration of multiple objectives, encompassing emissions, SFC, and component aging, remains an area warranting further exploration.

In this study, we present a new approach that combines two main innovations. First, we've created a multi-objective optimization model that considers fuel consumption, CO_2 and NOx emissions, and the degradation of FC and batteries. Then, building on this, we have developed a health-aware energy management strategy. Based on ECMS principles, this strategy aims to address the challenges posed by our optimization model in real-time, especially for vessels running on dual fuel in an all-electric mode.

II. MODELS DEVELOPMENT

The use case for this study is a fully electric yacht, originally operating with 4 diesel-generator sets, which is virtually retrofitted to the configuration displayed in Fig. 1. Two generator sets are replaced by hydrogen-fuelled FCs connected to the bus by DC/DC converters. The vessel is operated using a DC-distribution system. Two battery packs function as energy storage with a direct connection to the bus. Two generator sets remain in the layout to provide the required propulsive power, allowing for variable engine speed operation due to the AC/DC conversion.
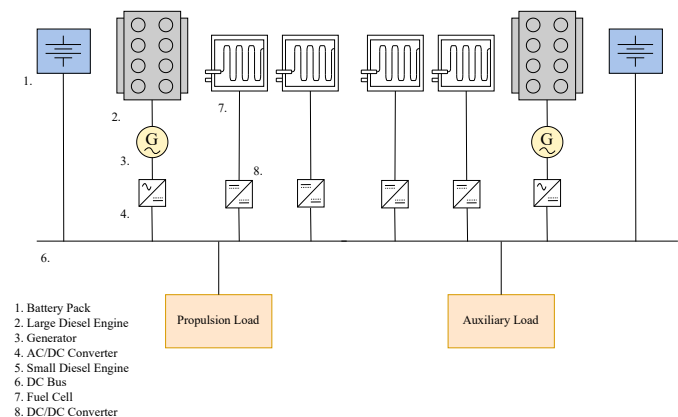

1. Battery Pack
2. Large Diesel Engine
3. Generator
4. AC/DC Converter
5. Small Diesel Engine
6. DC Bus
7. Fuel Cell
8. DC/DC Converter

Propulsion Load

Auxiliary Load

Fig. 1. Retrofitted layout of the yacht

TABLE I
CASE STUDY PARAMETERS

Parameter	Description	Value
V_{DC}	DC-bus voltage	$800 - 1000$ V
P_{Eng}	Engine power rating (x2)	1430 KWe
P_{FC}	FC power rating (x4)	217 KWe
E_{Bat}	Battery nominal capacity (x2)	2250 KWh
η_{AC-DC}	Conversion efficiency	0.98
η_{DC-AC}	Conversion efficiency	0.98
η_{DC-DC}	Conversion efficiency	0.98
η_m	Motor efficiency	0.97
η_{gb}	Gearbox loss	0.97
η_{gen}	Generator efficiency	0.96

Fig. 2. Specific fuel consumption map and NOx production map [20] of the engines.

A. Component Modelling

The propulsion system is modelled using mathematical relations of the steady-state behavior of the components or real-world measurements. In the following, the component models used are shortly introduced. The power system specifications are summarized in Tab. I. For the battery, we use a Lithium-Ion battery model based on Tremblay et al. [18], which we scale to the required size for the case study vessel. The battery is directly connected to the DC bus, which leads to an indirect control based on the power balance of the system. We model the ICE using maps for the SFC and the NOx over rpm and power for the complete performance envelope. Fig. 2 represents the SFC and NOx production maps. Notably, while CO_2 production exhibits a linear correlation with the fuel consumed, the NOx formation is related to the engine's operating conditions and cannot be related to the SFC. The engines are controlled with two parameters: the engine speed in rpm and the requested power. Those two parameters can be varied to use different operating points in the operational envelope presented in Fig. 2.

For the retrofit, a proton-exchange membrane FC is chosen. The FC is modelled after the publication of Souleman et al. [19]. A single cell is modelled and later combined into a stack of parallel and series cells of the required nominal power. The size is chosen to replace the nominal power of two diesel generators in the original vessel with four FC. The FC are controlled using a power reference, With this power reference, the required current, which is requested from the fuel cell, is determined. The system is further characterized by constant efficiencies for AC/DC (η_{AC-DC}), DC/AC (η_{DC-AC}), and DC/DC (η_{DC-DC}) converters and the losses of motor (η_m), gearbox (η_{gb}), and generators (η_{gen}). The values of the losses were obtained from information from manufacturers.

III. CONTROL DEVELOPMENT

The ECMS control framework is developed as a 2-level optimization. The first layer determines the optimal power scheduling of the components, and the second layer optimizes the operational points of the components in use. A set of variables describes the behaviour of the system in the controller. The five states, eight controls, and some additional inputs and parameters are shown in Tab. II.
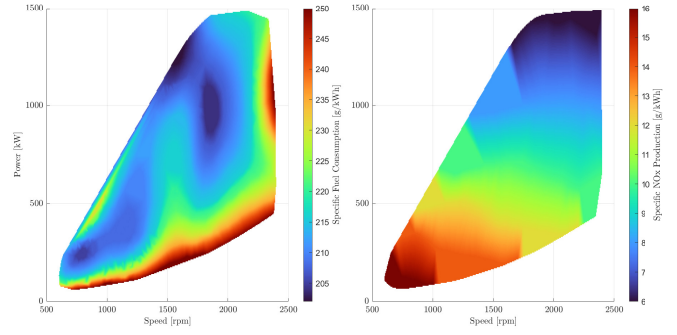
TABLE II
CONTROL VARIABLES AND PARAMETERS

Parameter	Description	Role	
I_{Eng}	Engine Current	State	x_1
I_{Load}	Requested Load Current	State	x_2
I_{FC}	Fuel Cell Current	State	x_3
I_{Bat}	Battery Current	State	x_4
SoC_{Bat}	Engine Current	State	x_5
$P_{Eng,i}$	i^{th} Engine Power Reference	Control	$u_i\ i \in \{1,2\}$
$n_{Eng,i}$	i^{th} Speed Reference	Control	$u_i\ i \in \{3,4\}$
$P_{FC,j}$	j^{th} Fuel Cell Power Reference	Control	$u_j\ j \in \{5,6,7,8\}$
P_{Prop}	Propulsion Load	Input	
P_{Aux}	Auxiliary Load	Input	
V_{DC}	DC Voltage	Input	
$V_{FC,i}$	Fuel Cell Voltage	Input	
r_{CO2}	Release Rate CO2 from Diesel	Param.	
n_s	Fuel Cell Cells in series	Param.	
F	Faraday constant	Param.	
p_D	Price of diesel	Param.	
p_{H2}	Price of hydrogen	Param.	
p_{Bat}	Equivalent factor battery	Param.	
n_p	Battery modules in parallel	Param.	
Q_{nom}	Battery nominal power	Param.	

The five states include the currents of sources and loads at the DC bus and the SoC of one battery since the behaviour of the batteries is identical due to the load sharing between them. The eight controls include the two variables for each engine, which are speed and power set points and the power set points for each fuel cell. The five states are reported in Eq. 1.

$$x_1 = \frac{(u_1 + u_2) \cdot \eta_{gen}}{V_{DC}} \cdot \eta_{AC-DC}$$
$$x_2 = \frac{P_{Prop} \cdot 1/\eta_{gb} \cdot 1/\eta_m + P_{Aux}}{V_{DC} \cdot \eta_{DC-AC}}$$
$$x_3 = \frac{(u_5 + u_6 + u_7 + u_8)}{V_{DC}} \cdot \eta_{DC-DC} \tag{1}$$
$$x_4 = x_1 + x_3 - x_2$$
$$x_5 = x_{5n-1} + \frac{1}{2}\frac{\Delta t \cdot x_4}{Q_{nom} \cdot n_p}$$

Those references for the state variables need to be matched by the controller's states to enforce the similarity to the real system. Objectives are defined to consider specific targets in the optimization. First, the SFC and the NOx formation of the

engines are related to the two control variables of each engine using the SFC and NOx production map of Fig. 2, For engines indexed by $i \in \{1, 2\}$, the relationships can be mathematically expressed as:

$$\text{SFC}_{\text{Eng,i}} = f_1(u_{2i-1}, u_{2i}) \qquad (2)$$
$$\text{NOx}_{\text{Eng,i}} = f_2(u_{2i-1}, u_{2i}) \qquad (3)$$

where f_1 and f_2 denote functions representing the SFC and NOx production rates, respectively.

With those references, the mass of diesel fuel consumed (m_D) and the emissions produced (m_{CO_2}, m_{NOx}) can be determined as follows:

$$m_D = \text{SFC}_{\text{Eng,1}} \cdot u_1 + \text{SFC}_{\text{Eng,2}} \cdot u_3 \qquad (4)$$
$$m_{CO_2} = \text{SFC}_{\text{Eng,1}} \cdot u_1 \cdot r_{CO2} + \text{SFC}_{\text{Eng,2}} \cdot u_3 \cdot r_{CO2} \quad (5)$$
$$m_{NOx} = \text{NOx}_{\text{Eng,1}} \cdot u_1 + \text{NOx}_{\text{Eng,2}} \cdot u_3 \qquad (6)$$

where r_{CO_2} is the release rate of CO_2 from diesel during combustion.

The mass of hydrogen utilized, m_{H2}, can be determined using the following relation:

$$m_{H2} = \left(\sum_{i=1}^{4} \frac{u_{4+i}}{V_{\text{FC},i}} \right) \cdot \frac{n_s}{F}, \qquad (7)$$

where n_s represents the number of cells in series within the fuel cell stack, $V_{\text{FC,i}}$ denotes the voltage of the ith fuel cell, and F is the Faraday constant.

According to Fig. 2, the SFC of the engines is not linear in the engine envelope; therefore, we define an efficiency in the following way

$$\eta_{\text{Eng}} = \frac{\text{SFC} - \text{SFC}_{\min}}{\text{SFC}_{\max} - \text{SFC}_{\min}}.$$

A. Objective Funtion Definition

To further diversify the control decision, we introduce four additional objectives C. The first three objectives primarily address the utilization of two distinct fuels (i.e., diesel and hydrogen) and batteries. Each objective correlates the consumed fuel mass to a specific pricing factor reflective of the fuel's market value. Notably, the first objective, which focuses on diesel consumption, incorporates the SFC relative to its optimal value. Concurrently, the battery power is equated with an equivalent factor, denoted as p_{Bat}. Finally, the fourth objective is defined as the amount of NOx emissions produced. The mathematical formulations of the four considered objectives are presented in Eq. 8

$$\begin{aligned} &C_1 : m_D \cdot p_D + \sum \eta_{\text{Eng,i}} \\ &C_2 : m_{H_2} \cdot p_{H_2} \\ &C_3 : P_{\text{Bat}} \cdot p_{\text{Bat}} \\ &C_4 : m_{NOx} \end{aligned} \qquad (8)$$

The objectives are normalized to compare objectives of different natures.

The health of the FCs is taken into account by introducing a lower limit at 20% of the load since degradation increases

and efficiency decreases below that limit due to starvation. In addition, the high price of hydrogen acts as a prevention against high currents on the FC and limits the degradation.

The battery health is taken into account by the battery objective, which penalizes the power output of the battery with the equivalent cost factor. Furthermore, constraints are imposed with boundaries to ensure that the operation remains between 20% and 80% of charge. The battery's depth of discharge (DoD) is also restricted to avoid excessive currents. This limitation is represented by the penalty term $c_{\text{Bat}} \cdot (x_4 - 0.5)$.

The scalarized objective function, also known as the cost function, can be formulated by considering the four distinct objectives of Eq. 8. Each objective has an associated weight denoted by λ_i with the index $i \in \{1, 2, 3, 4\}$.

$$J(\mathbf{x}, \mathbf{u}) = \sum \lambda_i \cdot C_i, \qquad (9)$$

where $\mathbf{x}$ and $\mathbf{u}$ represent the state and control variables, as reported in Tab. II.

B. Optimization Problem

Optimal vessel energy management is achieved by solving a multi-objective optimization problem. In this context, the objective function presented in Eq. 9 is enriched in two significant ways. Firstly, it integrates the controller's reference, denoted as $\mathbf{x}_{\text{ref}}$, which quantifies the deviations of the system's states from their desired or target values. Secondly, the objective function accounts for the DoD, indicating how much of the rechargeable battery's capacity has been utilized. The final objective function is reported in Eq. 10.

$$J(\mathbf{x}, \mathbf{u}) = (\mathbf{x} - \mathbf{x}_{\text{ref}}) + \text{DoD} + \sum \lambda_i \cdot C_i, \qquad (10)$$

Several constraints characterize the minimization problem described above. Foremost, we assert a power balance criterion, ensuring equivalence between requested and generated power:

$$P_{\text{Load}} = P_{\text{Gen}}. \qquad (11)$$

Operational bounds of distinct components are considered as:

$$\mathcal{O}_{\text{lower}} \leq \mathcal{O} \leq \mathcal{O}_{\text{upper}}. \qquad (12)$$

Where $\mathcal{O}$ symbolizes the operational level of a particular component with $\mathcal{O}_{\text{lower}}$ and $\mathcal{O}_{\text{upper}}$ designating the respective lower and upper operational confines. For the engine varieties under consideration, their operational envelopes are demarcated by nonlinear functions that prescribe both their upper and lower thresholds:

$$f_{\text{lower,i}}(\mathbf{x}) \leq \mathcal{O}_{\text{Eng,i}} \leq f_{\text{upper,i}}(\mathbf{x}) \qquad (13)$$

In this expression, $\mathcal{O}_{\text{Eng,i}}$ represents the operational magnitude of the ith engine, and $f_{\text{lower,i}}(\mathbf{x})$ and $f_{\text{upper,i}}(\mathbf{x})$ are nonlinear functions that respectively define the lower and upper operational perimeters.

Given the system dynamics and constraints, we aim to determine the optimal control input, $\mathbf{u}(\cdot|k)_{\text{opt}}$, that minimizes

the objective function J. Formally, the optimization problem can be articulated as:

$$\text{Minimize:} \quad J(\mathbf{u}(\cdot|k))$$
$$\text{s.t.:}$$
$$\begin{aligned} \mathbf{x}_{k+1} &= f(\mathbf{x}_k, \mathbf{u}_k) \\ \mathbf{u}_k &= \mathbf{u}_{k-1} + \Delta\mathbf{u}_k \\ g_{\text{in}}(\mathbf{x}_k, \mathbf{u}_k) &\leq 0 \\ g_{\text{eq}}(\mathbf{x}_k, \mathbf{u}_k) &= 0 \end{aligned} \quad (14)$$

where $\mathbf{x}_{k+1}$ represents the state at the next time-step as a function of the current state, $\mathbf{x}_k$, and the current control, $\mathbf{u}_k$ which is the evolution of the control input, which is derived by adjusting the control from the preceding time-step, $\mathbf{u}_{k-1}$, by an increment, $\Delta\mathbf{u}_k$.

The constraints ensure that g_{in} is an inequality function which, when evaluated with the current state and control, should always be non-positive, and g_{eq} represents the equality constraint which, for any valid state-control pairing, must evaluate to zero.

The optimization problem of Eq. (14) has a non-linear and non-convex objective and a series of non-linear constraints. In order to solve this problem, different approaches can be exploited [21]. A series of no-free-lunch theorems [22] ensure that there is no way to choose apriori the best optimization algorithms for a particular problem, and the only option is to empirically test multiple approaches verifying which is actually the best one. Nonetheless, in this case, we decided to apply Sequential Quadratic Programming (SQP) [23], supported by the other scholars' findings and results as reported in [24]. Moreover, based on the recent literature [25], this optimization algorithm reasonably covers the most important approaches to solving the optimization problem of Eq. (14). Since the starting point influences the convergence of all these algorithms, we employed a multi-start strategy [26]. In particular, as starting points, we used 100 random points uniformly distributed in the domain induced by the linear constraints of the optimization problem of Eq. (14). The optimization methods have been implemented using the Matlab 2023a environment.

It is worth noting that solving Eq. (14) for different values of λ_i in $[0, 1]$ allows for creating the so-called Pareto frontier in a computationally efficient way [27]. For this, we create a surface of feasible points between 0 and 1 for the four objectives. As base criteria for the selection of the weights, we use $\lambda_1 + \lambda_2 + \lambda_3 + \lambda_4 = 1$, which imposes the constraint that the sum of all values is required to be 1 at all times. Those objectives are the fuel used in the engine, the fuel used in the FCs, the equivalent cost of the battery, and the produced NOx emission. We optimize the minimization problem for every point of the Pareto front and compare the objective function value. As a first approach, we develop a holistic picking scheme. We chose the set of weights with the overall lowest objective function value for each step of the control. However, we disregard edge points, in which relevant objectives are set to zero.

The control is implemented as two-level optimization in a hierarchical approach. The first level schedules the combination of power sources to provide the load demand of every step, while the second level determines the exact operational points of every component by solving the minimization problem. The power source scheduling is based on the SOC of the batteries, the load demand, and the solution of the minimization problem for various constellations of power sources. The engines are used when the load demand exceeds a certain threshold. The controller takes the fluctuation of the load into account to suppress the constant changing of the control variables.

IV. SIMULATION STUDY

The control is tested in a simulation study with an example load profile and compared with a benchmark control. The example load profile covers $4\,\text{h}$ of operation, including times with and without sailing. Fig. 3 shows the load profile, where the auxiliary load is shown in red and the propulsion load in blue.

A. Benchmark

First, to evaluate the performance of the optimization controller, we develop a RBC as a benchmark. The RBC is designed to focus on providing the required load by generation scheduling while reducing the specific fuel consumption. For this, the batteries are used both to buffer fluctuation in the load and to allow the operation of the engines and FCs at fuel-efficient setpoints set along the propeller curve of the engine, which leads to the engine operating at fixed speeds. In Fig. 4, the concept of the RBC scheme is depicted. The inputs are the load demand of each step and the current SoC of the battery. The battery mode changes between charge and discharge when the SoC is approaching the lower or upper limit. The battery limits are chosen to 20% and 80% SoC, as this has been shown in practice to be beneficial for the lifetime. If no change of the battery mode is required and the load variation does not exceed 150 kW, the controller keeps the old set points for the next step to avoid excessive changes to the control variables. The set points of the engines and FCs are chosen to be the most fuel-efficient and with regard to the battery mode, the
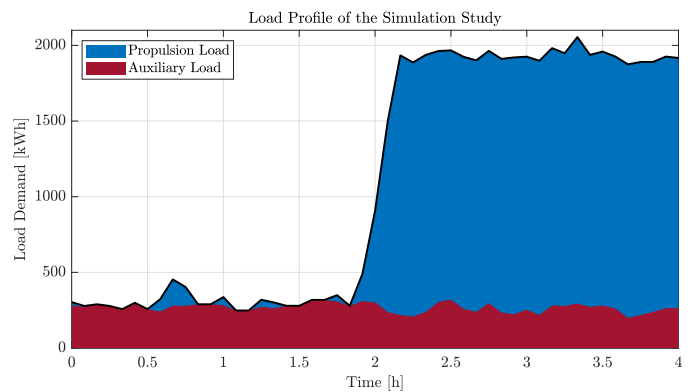
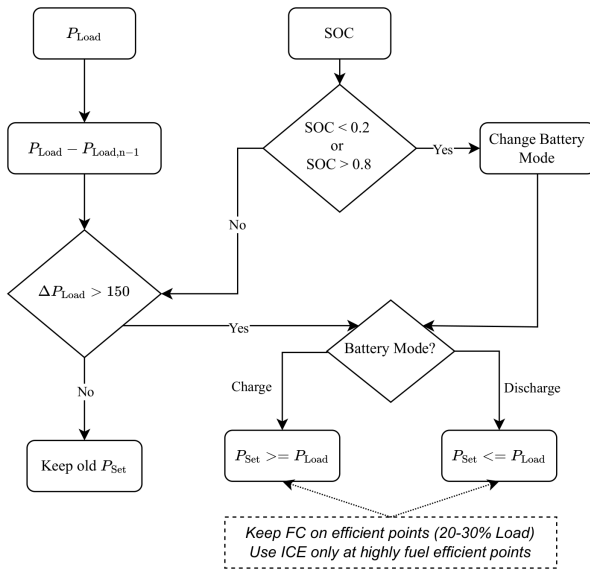Fig. 3. Load Profile used for the Simulation Study

Fig. 4. Schematic of the rule-based controller used as benchmark

Parameter	Description	Value
ρ_D	Density diesel	$0.838\,\mathrm{kg/l}$
r_{CO2}	CO2 release rate	$2.7\,\mathrm{t\ CO2/l}$
p_D	price diesel	$0.7\,\mathrm{Euro/l}$
p_{H2}	price hydrogen	$9.4\,\mathrm{Euro/kg}$
p_B	battery equivalent cost	$0.7\,\mathrm{Euro/l}$
c_{Bat}	battery penalty	3
SoC_0	Initial SoC	0.5

generated power is either $P_{\mathrm{Load}} \geq P_{\mathrm{Set}}$ or $P_{\mathrm{Load}} \leq P_{\mathrm{Set}}$. The RBC focuses on using the FCs at low loads to minimize the cost of hydrogen. We test the RBC on the load profile shown in Fig. 3. For the comparison, we choose the same discretization time as for the ECMS control, which is $5\,\mathrm{min}$. The smaller the timestep for the discretization is, the more it will resemble the real load profile shown in Fig. 3. Fig. 5 shows that the control secures the power balance over the complete operational time. It shows the balance of the currents of the three power sources in the first subplot and the load demand and the provided power in the second subplot. The RBC keeps the FC and the engines at stable setpoints while the battery is used to buffer for small changes in the load. The corresponding behaviour of the battery is shown in Fig. 6. The left axis shows the SoC over time, while the right axis displays the battery voltage. Since the batteries are directly connected to the bus, the voltage is also the voltage of the DC bus simultaneously.

B. ECMS Control

The performance of the ECMS controller is tested in a similar manner to the benchmark. The control step size is set to $5\,\mathrm{min}$. We assume the density of diesel according to [28], the release rate of CO2 from fuel r_{CO2} [29], and the price of the fuels for the control as shown in Tab. III. In this study, we assume the battery operates at the point of minimal fuel consumption of the engines to balance between the power sources. With all those parameters, the controller determines the values of the objectives and minimizes the cost function. Another factor to carefully choose is the penalty factor for the battery, which limits the DoD. A too-low factor increases the degradation due to high gradients, and a too-high factor will result in non-optimal use of the battery. This factor should be investigated using a logarithmic scale to determine a good choice between flexibility and health preservation. In this study, we tested only a few choices and showcased

the performance of the presented controller using a factor $c_{\mathrm{Bat}} = 3$, as a proof of concept. A full study on the effect of this parameter needs to be completed to be able to choose it optimally.

V. RESULTS

Fig. 7 shows the power balance of the produced energy and the required load, proving that the controller can provide the required load at every time step demand utilising all available power sources. Furthermore, the buffer inside the controller manages to ensure a not-too-high fluctuation in the control variables. Fig. 8 shows the corresponding DC system voltage and the SoC of the batteries. The control discharges the battery slowly allowing the FCs to operate a very efficient low load point for low load demand. The main propulsion load is provided using the engines, keeping the FCs at comparably low loads. We see, that the discharge current is not exceeding low values, which can have a beneficial aspect for the lifetime. Furthermore, the ECMS controller maintains the SoC within its respective limits. To assess our control's effectiveness, we compare the ECMS controller with the RBC. We demonstrate the ECMS controller's adaptability by examining its performance across various scenarios, that investigate the edges of the Pareto surface. The scenarios
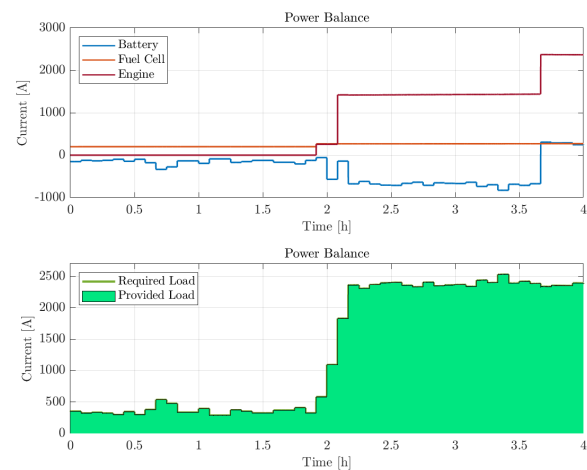

Fig. 5. Current sharing and power balance using rule-based control. The current colors indicate the power source (engines = red, FCs = orange, battery = blue, load = dark green and light green = sum of produced power)
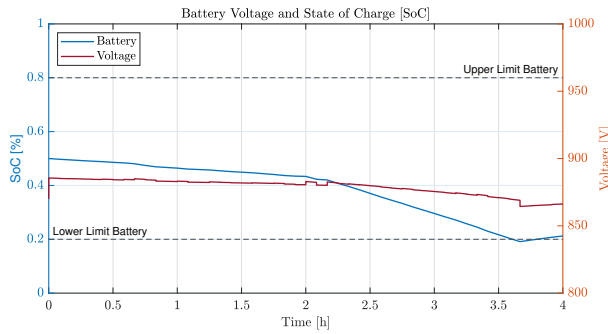
Fig. 6. Battery SoC and DC system voltage using rule-based control. SoC is shown in blue, Voltage in red.

Fig. 8. Battery SoC and DC system voltage using ECMS. SoC is shown in blue and Voltage in red.

TABLE IV
SCENARIO DESIGN

Scenario	Diesel	Hydrogen	Battery	NOx
	λ_1	λ_2	λ_3	λ_4
SFC	0.3	0.7	0	0
NOx	0	0	0	1

and their respective weights are displayed in Tab. IV. The first scenario takes into account the SFC for both fuels. Because hydrogen is more expensive and stored in smaller amounts than diesel, 30% focus is put on diesel and 70% on hydrogen consumption, The choice of this ratio is based on a small sensitivity analysis conducted beforehand. The second scenario focuses only on the reduction of NOx emissions. In the third scenario, we compare the holistically optimal combination of objective weights determined with the Pareto front presented in the previous section. The results of the tested scenarios for the ECMS controller and the RBC are shown in Tab. V. We compare five aspects: diesel consumption, hydrogen consumption, CO_2 production, NOx production, and

overall costs. We calculate the deviation from the RBC results for each aspect to showcase the ECMS controller's performance on different objectives. We observe that the ECMS controller's performance differs between the scenarios, and the results correspond to the focus of the objectives. A focus on emission production results in an increase in hydrogen consumption, a decrease in diesel consumption, and increased fuel cost. The test of the NOx scenario shows that a drastic decrease in NOx formation is possible by choice of engine operation point and usage of more hydrogen. A focus on the reduction of the consumed fuel results in decreasing hydrogen and increasing diesel consumption, which the higher price of hydrogen can explain. However, the test of this scenario shows that it is hard to beat a well-designed RBC for a single objective optimization. An increase in NOx formation can be observed, as the objective is not prioritized in this scenario.

The Pareto front scenario results show an overall balanced performance. While we see an increase in diesel consumption, we still see a decrease of nearly 5% in the formation of NOx emission, which can be related to the choice of the operational point. In addition, the controller is able to save some hydrogen, which results in only an increase of 7.36% of the overall cost. In conclusion, the ECMS framework provides a stable trade-off for different scenarios and acts as expected, as it is not possible to minimize contradicting objectives all at the same time. Moreover, with this ECMS framework, we allow users to express their preferences and prioritize different aspects of the operation. Finally, the penalty on the DoD of the batteries and the continuous running of the FCs at a base load introduces
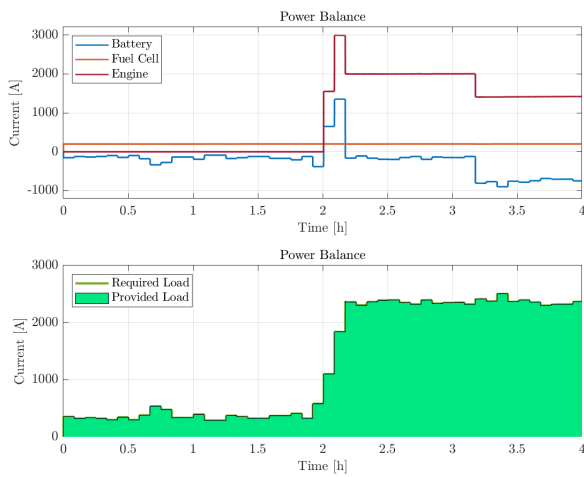

Fig. 7. Current sharing and power balance using ECMS. The current colors indicate the power source (engines = red, FCs = orange, battery = blue, load = dark green and light green = sum of produced power)
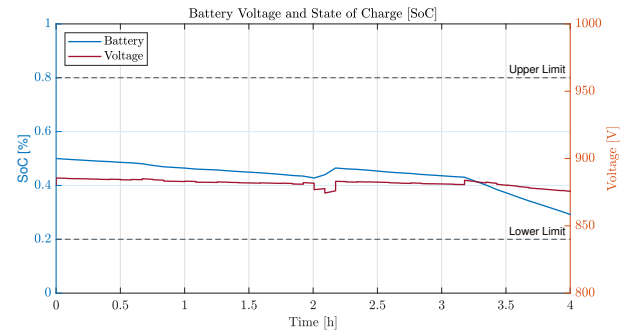
TABLE V
SCENARIO COMPARISON

Scenario	Fuel		Emission		Cost
	Diesel	Hydrogen	CO_2	NOx	
RBC	0.626 [t]	0.039 [t]	2.01 [t]	0.026 [t]	889.4 [€]
SFC	0.773 [t]	0.034 [t]	2.49 [t]	0.03 [t]	967 [€]
	+23.4%	-12.7 [%]	+23.9 [%]	+14.5 [%]	+8.7 [%]
NOx	0.354 [t]	0.148 [t]	1.14 [t]	0.010 [t]	1684 [€]
	-43.5[%]	+277 [%]	-43.2 [%]	-59.9 [%]	+89.4 [%]
Pareto	0.758 [t]	0.034 [t]	2.44 [t]	0.025 [t]	954 [€]
	+21.1 [%]	-12.7 [%]	+21.6 [%]	-4.7 [%]	+7.4 [%]

health-awareness into the control.

VI. Conclusion

This paper presented the first proof of concept of an optimization-based control using equivalent consumption minimization for a multi-component vessel energy system. The developed controller fulfills the required load demand and stabilizes the system while considering the fuel consumption of two different fuels and the produced NO_x emissions. The degradation of batteries and FCs was considered by choosing operation limits and penalizing the use of the component, introducing health-awareness into the control. The controller was able to optimize between using the emission-free, but expensive hydrogen and less expensive, but emission-producing diesel in three test scenarios. As a first step, we demonstrated the application on a $4\,\text{h}$ load profile from a real vessel and showcase potential for flexible adaption of the performance based on the choice of the weights of the multi-objective problem. Future work will focus on implementing degradation models for the batteries and fuel cells into the model and the control strategy toward enhanced health-aware control. In addition, a study of the DoD penalization should be conducted to obtain insights on optimally choosing it. This also applies to the choice of the equivalent cost of the battery use, which could be chosen adaptively in the future. Furthermore, variable component efficiencies are a way to improve the model's accuracy compared to the real system. In addition, the focus can be set on developing an advanced selection scheme for the Pareto front weights to highlight the potential of influencing the control as an operator.

References

[1] J. F. Hansen and F. Wendt, "History and State of the Art in Commercial Electric Ship Propulsion, Integrated Power Systems, and Future Trends," *Proceedings of the IEEE*, vol. 103, no. 12, pp. 2229–2242, Dec. 2015.

[2] V. Eyring, H. W. Köhler, A. Lauer, and B. Lemper, "Emissions from international shipping: 2. Impact of future technologies on scenarios until 2050," *Journal of Geophysical Research: Atmospheres*, vol. 110, no. D17, 2005.

[3] C. Nuchturee, T. Li, and H. Xia, "Energy efficiency of integrated electric propulsion for ships – A review," *Renewable and Sustainable Energy Reviews*, vol. 134, p. 110145, Dec. 2020.

[4] P. Nema, R. K. Nema, and S. Rangnekar, "A current and future state of art development of hybrid energy system using wind and PV-solar: A review," *Renewable and Sustainable Energy Reviews*, vol. 13, no. 8, pp. 2096–2103, Oct. 2009.

[5] A. D. Korberg, S. Brynolf, M. Grahn, and I. R. Skov, "Techno-economic assessment of advanced fuels and propulsion systems in future fossil-free ships," *Renewable and Sustainable Energy Reviews*, vol. 142, p. 110861, May 2021.

[6] M. Perčić, I. Ančić, and N. Vladimir, "Life-cycle cost assessments of different power system configurations to reduce the carbon footprint in the Croatian short-sea shipping sector," *Renewable and Sustainable Energy Reviews*, vol. 131, p. 110028, Oct. 2020.

[7] S. Atilhan, S. Park, M. M. El-Halwagi, M. Atilhan, M. Moore, and R. B. Nielsen, "Green hydrogen as an alternative fuel for the shipping industry," *Current Opinion in Chemical Engineering*, vol. 31, p. 100668, Mar. 2021.

[8] M. Prussi, N. Scarlat, M. Acciaro, and V. Kosmas, "Potential and limiting factors in the use of alternative fuels in the European maritime sector," *Journal of Cleaner Production*, vol. 291, p. 125849, Apr. 2021.

[9] M. Banaei, J. Boudjadar, and M.-H. Khooban, "Stochastic Model Predictive Energy Management in Hybrid Emission-Free Modern Maritime Vessels," *IEEE Transactions on Industrial Informatics*, vol. 17, no. 8, pp. 5430–5440, Aug. 2021.

[10] N. Collath, B. Tepe, S. Englberger, A. Jossen, and H. Hesse, "Aging aware operation of lithium-ion battery energy storage systems: A review," *Journal of Energy Storage*, vol. 55, p. 105634, 2022.

[11] X. Tang, T. Jia, X. Hu, Y. Huang, Z. Deng, and H. Pu, "Naturalistic Data-Driven Predictive Energy Management for Plug-In Hybrid Electric Vehicles," *IEEE Transactions on Transportation Electrification*, vol. 7, no. 2, pp. 497–508, Jun. 2021.

[12] S. Fang, Y. Xu, Z. Li, T. Zhao, and H. Wang, "Two-Step Multi-Objective Management of Hybrid Energy Storage System in All-Electric Ship Microgrids," *IEEE Transactions on Vehicular Technology*, vol. 68, no. 4, pp. 3361–3373, Apr. 2019.

[13] J. Drgoňa, J. Arroyo, I. Cupeiro Figueroa, D. Blum, K. Arendt, D. Kim, E. P. Ollé, J. Oravec, M. Wetter, D. L. Vrabie, and L. Helsen, "All you need to know about model predictive control for buildings," *Annual Reviews in Control*, vol. 50, pp. 190–232, 2020.

[14] A. Haseltalab and R. R. Negenborn, "Model predictive maneuvering control and energy management for all-electric autonomous ships," *Applied Energy*, vol. 251, p. 113308, Oct. 2019.

[15] D. Sturzenegger, D. Gyalistras, M. Morari, and R. S. Smith, "Model Predictive Climate Control of a Swiss Office Building: Implementation, Results, and Cost–Benefit Analysis," *IEEE Transactions on Control Systems Technology*, vol. 24, no. 1, pp. 1–12, Jan. 2016.

[16] H. Li, A. Ravey, A. N'Diaye, and A. Djerdir, "A novel equivalent consumption minimization strategy for hybrid electric vehicle powered by fuel cell, battery and supercapacitor," *Journal of Power Sources*, vol. 395, pp. 262–270, Aug. 2018.

[17] M. Kalikatzarakis, R. D. Geertsma, E. J. Boonen, K. Visser, and R. R. Negenborn, "Ship energy management for hybrid propulsion and power supply with shore charging," *Control Engineering Practice*, vol. 76, pp. 133–154, Jul. 2018.

[18] O. Tremblay, L.-A. Dessaint, and A.-I. Dekkiche, "A Generic Battery Model for the Dynamic Simulation of Hybrid Electric Vehicles," in *2007 IEEE Vehicle Power and Propulsion Conference*, Sep. 2007, pp. 284–289.

[19] N. M. Souleman, O. Tremblay, and L.-A. Dessaint, "A generic fuel cell model for the simulation of Fuel Cell Power Systems," in *2009 IEEE Power & Energy Society General Meeting*, Jul. 2009, pp. 1–8.

[20] R. D. Geertsma, R. R. Negenborn, K. Visser, and J. J. Hopman, "Design and control of hybrid power and propulsion systems for smart ships: A review of developments," *Applied Energy*, vol. 194, pp. 30–54, May 2017.

[21] M. J. Kochenderfer and T. A. Wheeler, *Algorithms for decision making*. Mit Press, 2022, https://algorithmsbook.com/.

[22] D. H. Wolpert and W. G. Macready, "No free lunch theorems for optimization," *IEEE transactions on evolutionary computation*, vol. 1, no. 1, pp. 67–82, 1997.

[23] P. T. Boggs and J. W. Tolle, "Sequential quadratic programming," *Acta numerica*, vol. 4, pp. 1–51, 1995.

[24] S. Mennen, F. P. Willems, and M. Donkers, "A sequential quadratic programming approach to combined energy and emission management of a heavy-duty parallel-hybrid vehicle," *IFAC-PapersOnLine*, vol. 55, no. 24, pp. 335–341, 2022.

[25] Z. Khalik, G. Padilla, T. Romijn, and M. Donkers, "Vehicle energy management with ecodriving: A sequential quadratic programming approach with dual decomposition," in *2018 Annual American Control Conference (ACC)*. IEEE, 2018, pp. 4002–4007.

[26] R. Martí, "Multi-start methods," in *Handbook of Metaheuristics*, 2003.

[27] M. Emmerich and A. H. Deutz, "A tutorial on multiobjective optimization: fundamentals and evolutionary methods," *Natural computing*, vol. 17, no. 3, pp. 585–609, 2018.

[28] F. Murphy, K. McDonnell, E. Butler, and G. Devlin, "The evaluation of viscosity and density of blends of Cyn-diesel pyrolysis fuel with conventional diesel fuel in relation to compliance with fuel specifications EN 590:2009," *Fuel*, vol. 91, no. 1, pp. 112–118, Jan. 2012.

[29] A. Q. Jakhrani, A. R. H. Rigit, A.-K. Othman, S. R. Samo, and S. A. Kamboh, "Estimation of carbon footprints from diesel generator emissions," in *2012 International Conference on Green and Ubiquitous Technology*, Jul. 2012, pp. 78–81.